Electronic structure and properties of EuO and EuS in the molecular-cluster approximation*

E. Byrom, D. E. Ellis, and A. J. Freeman
Department of Physics, Northwestern University, Evanston, Illinois 60201
(Received 23 February 1976)

Molecular-cluster models are developed to describe ground-state properties of EuO and EuS in the Hartree-Fock-Slater one-electron approximation. Spin-polarized $(EuX_6)^{10-}$ complexes are examined using both neutral- and ionic-model potentials which incorporate a part of the effect of the crystalline environment. Self-consistent calculations are made for $(EuO_6)^{10-}$. From the charge and spin densities, the transferred hyperfine field at the O site in EuO is found to be -8 ± 2 kG and a small solid-state bonding effect is predicted for the neutron magnetic form factor. The pressure dependence of the charge density at the Eu nucleus in EuS is determined as a function of bond length in the $(EuS_6)^{10-}$ cluster and used to obtain from the experimental data an isomer-shift calibration constant $\alpha = -0.48 a_0^3$ mm/sec. The one-electron energy levels of the $(EuO_6)^{10-}$ cluster are found to be in good agreement with the augmented-plane-wave results of Cho when both calculations are performed with similar model potentials. The extension to self-consistency leads to significant energy-level rearrangement which indicates the importance of final-state relaxation and Coulomb correlation effects in the interpretation of experimental spectra.

I. INTRODUCTION

The europium chalcogenides EuX (X = O, S, Se, and Te), an important class of magnetic semiconductors, have magnetic ordering properties which vary from ferromagnetic (EuO) to antiferromagnetic (EuTe), and exhibit a red shift in their optical spectra with increasing magnetic order. Insulators in the pure state, they become semiconducting when doped with rare-earth impurities, and show large negative magnetoresistances near their transition temperatures. A review of the experimental properties and of the theoretical interpretations has been given by Methfessel and Mattis.[1] The general picture which has emerged is one of magnetic moments localized on Eu^{2+} ions with a high-spin configuration $(4f\uparrow)^7(4f\downarrow)^0$. These moments are coupled by an antiferromagnetic 180° superexchange interaction, acting through the X^{2-} ligand ions, and by a ferromagnetic exchange which depends on the covalent mixing of Eu $4f$ orbitals with the unoccupied $5d$ orbitals on nearest-neighbor Eu sites. Now most rare earths are trivalent yielding, in their respective monochalcogenides, two electrons to the ligand ion, and one to the conduction band, so that the compounds are metallic. Added as impurities to the insulating Eu chalcogenides, rare-earth ions populate the conduction band with a fraction of their third valence electrons. Since the conduction band is involved in magnetic ordering (as shown by the magneto-optical red shift, and as expected from the nature of the ferromagnetic interaction), the phenomena associated with the magnetic phase transition are modified and the negative magnetoresistance effects are obtained. More detailed elucidation of these effects has been attempted in terms of both impurity and energy-band models,[1] but no complete theory can be said to have been found.

The spin-polarized one-electron theory has been quite successfully applied in interpreting magnetic properties, optical data, and photoemission spectra of lighter materials, notably the $3d$ metals and their compounds. While the limitations of such a model are evident, for example, in their inability to predict correctly multiplet splittings observed, it is clearly worthwhile to investigate their applicability to open-shell rare-earth systems.

This paper describes the results of theoretical molecular-cluster calculations for EuO and EuS in the Hartree-Fock-Slater (HFS) approximation. Both model-potential and self-consistent studies are undertaken to better understand the role of "localized" $4f$ electrons in the bonding and magnetic interactions of rare-earth compounds. Several ground-state properties of these systems, notably charge and spin densities, are used to determine such experimental properties as neutron magnetic form factors and transferred hyperfine fields. Results for the pressure dependence of the electron density at the Eu nucleus in EuS are used in conjunction with the experimental Mössbauer isomer-shift data of Kalvius *et al.*[2] to determine α, the isomer-shift calibration constant, for ^{151}Eu.

As is well known, parametrized band-structure models[3,4] have been presented which are compatible with a one-electron interpretation of optical, x-ray, photoemission, and magnetic data for the europium chalcogenides. Thus, the applicability of the one-electron HFS model to the description of some of these excited-state properties is also tested in this work, with special attention to $4f$

excitation processes. It is found that non-self-consistent cluster models can produce an essentially identical picture to that obtained by the parametrized band schemes. However, a self-consistent calculation of the ground-state eigenvalues destroys this apparent agreement between theory and observed spectra. The reasons are clear even for free-atom systems. Because of the high degree of localization of the $4f$ electrons, a correct interpretation of the data requires the inclusion of intra-atomic Coulomb correlation effects in total-energy calculations of the different configuration states involved in the observed transitions. Such calculations are at present practical only for isolated atoms or ions.

II. DISCRETE VARIATIONAL METHOD FOR THE SOLUTION OF THE SPIN-UNRESTRICTED HFS EQUATIONS

In this work, the spin-unrestricted Hartree-Fock-Slater (HFS) equations are solved for all the electrons in a molecular cluster of Eu^{2+} and its six nearest-neighbor ligand ions, arranged in an octahedron (O_h point-group symmetry). In this approach, the Hartree-Fock (HF) one-electron equations

$$H\psi = (-\tfrac{1}{2}\nabla^2 + V_{\text{Coulomb}} + V_{\text{ex}})\psi = \epsilon\psi \tag{1}$$

are modified by replacing the nonlocal exchange operator V_{ex} by a local average, further approximated to

$$V_{\text{ex},\sigma}(\vec{\mathbf{r}}) = -3\alpha[(3/4\pi)\rho_\sigma(\vec{\mathbf{r}})]^{1/3}, \tag{2}$$

where σ refers to the spin state. By applying different criteria in the approximation,[5] α may be derived as either $\frac{2}{3}$ or 1; it has been common practice to choose a value between these two extremes for best agreement with some relevant HF or experimental result. In this paper, the effects of different values of α will be considered, but no attempt will be made to adjust α to fit to experiment.

The wave functions are obtained in terms of a linear-combination-of-atomic-orbitals basis set,

$$\psi_i(\vec{\mathbf{r}}) = \sum_j A_j(\vec{\mathbf{r}})\, C_{ji} \tag{3}$$

by the discrete variational method (DVM) which has been described in detail elsewhere.[6] An error functional for eigenfunction i at point $\vec{\mathbf{r}}$ is defined as

$$\delta_i(\vec{\mathbf{r}}) = (H - \epsilon_i)\,\psi_i(\vec{\mathbf{r}}) \tag{4}$$

and the coefficients C_{ji} are determined by minimizing a weighted average of $\delta_i(\vec{\mathbf{r}})$ over a discrete set of sample points. A secular equation is derived, identical to the Rayleigh-Ritz equation,

$$\underline{H}\underline{C} = \underline{S}\underline{C}E, \tag{5}$$

but with matrix elements given in discrete form. The choice of sample points corresponds to a statistical form of numerical integration. The $A_j(\vec{\mathbf{r}})$ are taken to be Slater-type orbitals (STO's) centered on both the Eu and ligand ions, giving a basis set of double zeta quality (see Table I). Matrix elements H_{kj} and S_{kj} of the Hamiltonian and overlap matrices are evaluated by summing over a grid of 4000 sample points. The HFS equations [Eq. (1)] are thus solved approximately once a charge density $\rho(\vec{\mathbf{r}})$ has been determined. The initial $\rho(\vec{\mathbf{r}})$ is a sum of spherically symmetric charge densities. For self-consistent iterations, V_{Coulomb} is derived from a $\rho(\vec{\mathbf{r}})$ partitioned into overlapping spherical distributions; while V_{ex} is taken from the $\frac{1}{3}$ power of the unpartitioned $\rho(\vec{\mathbf{r}})$. The sensitivity of one-electron results to the choice of model potential, ranging from a free-atom charge-density potential to an approximately self-consistent potential for the cluster embedded in its crystalline environment, is studied.

III. FREE-ATOM-ION SUPERPOSITION MODELS

The systems $(EuO_6)^{10-}$ and $(EuS_6)^{10-}$ were treated first as isolated clusters, in a potential generated from the superposed charge and spin densities of free Eu and O (or S) atoms centered on the cluster sites, that is

$$\rho(\vec{\mathbf{r}}) = \sum_{\nu=1}^{7} \rho_\nu(|\vec{\mathbf{r}} - \vec{\mathbf{R}}_\nu|)\,. \tag{6}$$

The Eu–O bond length was taken as $4.8619a_0$ and the equilibrium Eu–S distance as $5.64a_0$.[7,8] In further calculations for $(EuO_6)^{10-}$, a part of the effect of the crystal environment experienced by the cluster is included in the model potential. This is done in one of two ways. The "neutral" crystal potential was generated from free-atom charge densities located at every site in the crystal. The portion of the resulting Coulomb potential due to sites outside the cluster is illustrated in Fig. 1. (The summation was actually carried out only for those atoms within a finite radius of the cluster: the ripples in the curves in Fig. 1 indicate that the summation did not include quite enough atoms.) A second, or "ionic," crystal potential was generated from Eu^{2+} and O^{2-} free-ion charge densities, together with a point-ion Coulomb potential (the Madelung potential). The total "ionic" Coulomb potential, with the contributions of the cluster sites subtracted out, is shown in Fig. 2. Although it is convenient to separate the Coulomb potential into "cluster" and "exterior" contributions, it is not possible similarly to partition the exchange potential [Eq. (2)]. The model

TABLE I. Slater-type-orbital basis sets for Eu chalcogenide clusters.

Europium				Oxygen (Ref. 32)		Sulfur (Ref. 32)	
Primary basis set (Ref. 10)		Expanded *s* basis [a]					
ln	ζ	ln	ζ	ln	ζ	ln	ζ
*s*1	62.7	*s*1	100.0	*s*1	10.1085	*s*1	17.6913
2	31.785	1	62.7	1	7.062 27	1	13.7174
3	35.7	1	38.46	2	2.621 58	2	7.0
3	16.703	2	45.0	2	1.627 05	2	4.5
4	16.596	2	28.57	*p*2	3.681 27	3	3.159 55
4	9.159	3	30.0	2	1.653 72	3	1.815 13
5	8.533	3	16.6			*p*2	8.902 62
5	3.718	4	16.6			2	4.907 27
5	2.24	4	9.159			3	2.333 68
		5	3.718			3	1.321 71
*p*2	30.703	5	8.553				
3	35.7	6	2.69				
3	17.292	6	1.5				
4	15.904						
4	8.911						
5	8.43						
5	3.496						
5	2.019						
*d*3	21.612						
3	13.95						
4	8.694						
4	5.829						
*f*4	11.764						
4	6.603						
4	4.402						
4	2.416						
*d*5	3.718 [b]						
5	2.24 [b]						

[a] Used for EuS isomer shift calculations.
[b] Not included in all calculations.

potential is that of the complete periodic solid, as required for a band-structure calculation. The cluster levels in this potential bear a close resemblance to the corresponding band structures. However, in order to construct a fully consistent model one must take account of Pauli exclusion between occupied cluster states and "exterior" states. Such refinements have not been included in the present calculations; some work has been done on a parametrized pseudopotential approach for metal clusters.[9]

The stability of the eigenvalues with respect to

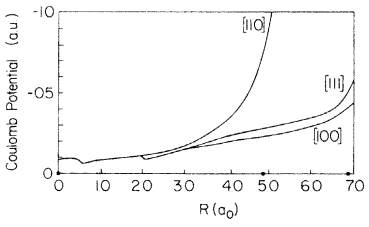

FIG. 1. "Neutral" crystal potential showing the contribution to the Coulomb potential from sites outside the cluster along different crystal directions. Note that, away from the cluster, the crystal potential is periodic.

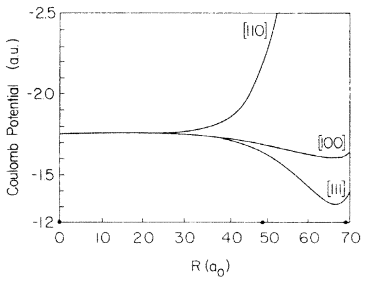

FIG. 2. "Ionic" crystal potential showing the contribution to the Coulomb potential from sites outside the cluster along different crystal directions.

TABLE II. Core eigenvalues (spin up) and spin splittings $\epsilon\uparrow-\epsilon\downarrow$ in a.u. for the Eu^{2+} free ion and the $(EuO_6)^{10-}$ cluster for $\alpha=0.7$.

	Free ion $\epsilon\uparrow$			Cluster			
				Ionic model potential		SCF results	
	Numerical wave functions	HFS-DVM	$\Delta\epsilon$	$\epsilon\uparrow$	$\Delta\epsilon$	$\epsilon\uparrow$	$\Delta\epsilon$
1*s*	1673.71	1673.19		1672.54		1673.14	
2*s*	265.93	265.75		265.01		265.42	
2*p*	252.94	252.93		252.23		252.76	
3*s*	58.66	58.64	0.12	57.93	0.12	57.95	0.12
3*p*	52.88	52.87	0.12	52.16	0.11	52.21	0.11
3*d*	42.05	42.07	0.08	41.38	0.08	41.40	0.08
4*s*	11.86	11.85	0.24	11.14	0.24	11.03	0.23
4*p*	9.62	9.59	0.24	8.89	0.24	8.79	0.23
4*d*	5.62	5.62	0.24	4.91	0.24	4.81	0.23

reasonable changes in the integration mesh is 0.01 Hartree atomic units (a.u.) or better. It has been shown[10] that the use of the STO basis set of Table I in Eu^{2+} free-ion variational calculations gives eigenvalues differing from those for exact numerical HF wave functions by ≤ 0.03 a.u. In Table II, the core eigenvalues and spin splittings of two Eu^{2+} free-ion HFS ($\alpha=0.7$) calculations are compared: the difference between the exact HFS numerical-wave function and DVM treatments is ≤ 0.03 a.u. except for the "deep core" Eu 1*s* and 2*s* levels [which requires large numbers of sample points in the core region for accurate treatment (see Sec. V)]. The differences between the Eu-core levels in the free ion and in the various cluster-model potentials may be described as uniform overall shifts. These are due partly to electrostatic shifts of the zero of energy and partly to incomplete convergence of the sampling scheme.

When a double zeta basis set is used, it is not possible to express covalent mixing by means of a single coefficient. The molecular orbitals contain contributions which resemble free-atom orbitals, but those orbitals are not only mixed, but are also altered somewhat in shape. The covalent effects cannot be attributed to any one pair of orbitals, since small mixings appear in all possible cases (listed in Table III). The total densities must be studied directly in assessing covalent effects.

Contour maps of the $(EuO_6)^{10-}$ cluster spin density in the "ionic" crystal potential are shown in Figs. 3 and 4. In these figures, the contours are plotted in two planes. One plane includes a bond axis [100] and a face diagonal of a cubic unit cell [110]. The other contains the same [110] axis, a body diagonal [111], and a second bond axis [001]. An inset shows the spin density plotted along the bond axis near the O site. Further calculations with increased exchange show that all the major features are exaggerated in the $\alpha=1$ case (Fig. 3) compared to the $\alpha=0.7$ calculation (Fig. 4): the density at the Eu nucleus is more negative; the peak in the region of the maximum of the 4*f* function is higher; the density at the O nucleus is also more negative, and a region of negative density appears around the Eu ion. The increased height of the 4*f* peak follows from the altered shape of the 4*f* radial function, illustrated in Fig. 5 for the a_{2u} molecular orbital (pure 4*f* character) in the two exchange potentials. The asymmetric form of the spin density about the O site arises from the mixing of O *s* and *p* functions in the same molecular orbitals. The mixing is due to the low bonding symmetry at the O site in the cluster, where the O orbitals are allowed to bond with Eu orbitals on only one of the six adjacent Eu sites.

TABLE III. Atomic character and molecular symmetry in EuX_6 clusters.

In the representation of the O_h point group	Metal orbitals	May mix with ligand orbitals
a_{1g}	*s*	*s*, *p*
e_g	*d*	*s*, *p*
t_{1g}		*p*
t_{2g}	*d*	*p*
a_{2u}	*f*	
t_{1u}	*p*, *f*	*s*, $p\sigma$, $p\pi$
t_{2u}	*f*	*p*

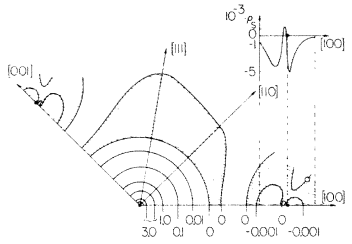

FIG. 3. Spin-density contours plotted in two planes for the $(EuO_6)^{10-}$ cluster in the "ionic" crystal potential, with $\alpha = 1.0$. One plane includes the [100] and [110] axes of the cluster; the other includes the [110], [111], and [001] axes. Inset: the spin density along the [100] axis, near the O site.

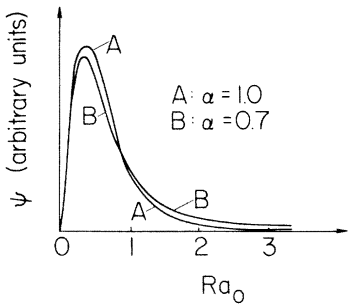

FIG. 5. $1a_{2u}\downarrow$ molecular orbital in the "ionic" crystal potential, plotted along the bond axis for two values of α (in calculation A, $\alpha = 1.0$ and in B, $\alpha = 0.7$). This orbital contains only $4f$ basis functions.

The mixing can be wholly avoided only at the price of using a much larger cluster.

The spin density at the O nucleus gives rise to a magnetic field which generates a hyperfine structure accessible by magnetic resonance techniques in the case of those O isotopes that have a nuclear magnetic moment. This is the isotropic part of the transferred hyperfine field, which has been measured by ^{19}F electron-nuclear double resonance for CaF_2:Eu (as -2.0 kG),[11] but not for EuO. In the "neutral" crystal potential, the cluster spin density at the O nucleus is $-0.015a_0^{-3}$ (corresponding to a magnetic field of -7 kG). Calculations were also performed for an oxygen atom embedded in the same potential, giving a spin density at its nucleus of $-0.012a_0^{-3}$. In the "ionic" crystal potential, the density is $-0.003a_0^{-3}$ for $\alpha = 1$. This suggests that the larger value for the "neutral" crystal potential arises from the polarization of the O ion by an exchange potential from the Eu $6s$ electrons.

IV. SELF-CONSISTENT-FIELD CALCULATIONS

It has already been noted that small admixtures of all basis functions allowed by Table III are present in all the eigenfunctions. Large mixings, or hybridization are also allowed. Since a unitary transformation upon the occupied orbitals of a

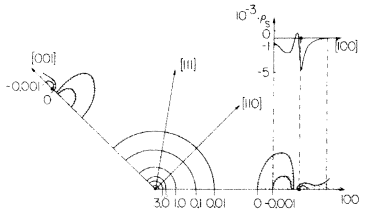

FIG. 4. Spin-density contours for the $(EuO_6)^{10-}$ cluster in the "ionic" crystal potential, with $\alpha = 0.7$ (cf. caption of Fig. 3).

Slater determinant wave function can produce no change in the densities, linear combinations of two occupied molecular orbitals may occur. Such large mixings are present in these results, as artifacts of the matrix diagonalization procedure, when eigenvalues are almost degenerate. But in non-self-consistent HFS calculations there is no distinction between occupied and unoccupied orbitals. Degenerate mixing between, e.g., occupied $2p\downarrow$ and unoccupied $4f\downarrow$ orbitals does change the densities, and in an undesirable way. Any reasonable choice of occupation numbers leads to a large contribution to the spin-down charge density in the vicinity of the maximum of the $4f$ function, and thus to an unphysical reduction of the spin density there. The desired occupation can only be enforced in a convergent self-consistent-field (SCF) solution. An iteration of the results to self-consistency was undertaken for the $(EuO_6)^{10-}$ cluster with $\alpha = 0.7$. Since the converged $(EuO_6)^{10-}$ cluster solution is expected to be close to the Eu^{2+}, O^{2-} ionic configuration, free-ion charge densities were used to start the calculation, and occupation numbers were chosen to enforce the full (10–) cluster charge at each iteration. Since so ionic a cluster is unbound in isolation, i.e., charge density will tend to move to regions as far from the cluster as the basis set allows, a stabilizing potential from the surrounding crystal was included in the calculation (see Fig. 2). The total potential for spin σ at any iteration is

$$V_\sigma = V_{\text{Coulomb}}(\text{cluster}) + V_{\text{Coulomb}}(\text{external}) - 3\alpha(3/4\pi)^{1/3}[\rho_\sigma(\text{cluster}) + \rho_\sigma(\text{external})]^{1/3}, \quad (7)$$

with $V_{\text{Coulomb}}(\text{cluster})$ and $\rho_\sigma(\text{cluster})$ generated from the wave functions of previous iterations, and $V_{\text{Coulomb}}(\text{external})$ and $\rho_\sigma(\text{external})$ kept constant throughout.

The principal difficulty in performing self-con-

sistent spin unrestricted calculations lies in stabilizing a particular molecular-orbital configuration. Since molecular orbitals are, in general, mixtures of basis functions on more than one site, the alterations in the coefficients of the basis functions from one iteration to the next may result in sizable charge transfer from one site to another. It is expected that, as self-consistency is approached, the changes from one cycle to the next will diminish, but in the early stages of the iteration procedure, the changes may be so drastic as to prevent the approach to a self-consistent solution.

In the case of $(EuO_6)^{10-}$, it was noted that the energy of the $1a_{2u}\downarrow$ molecular orbital (pure $4f$ character) was on some iteractions below and on others above that of the $1t_{1g}\downarrow$ orbital (pure ligand $2p$ character). Since both $4f$ and $2p$ orbitals occur in the t_{1u} and t_{2u} representations, it follows that, e.g., the $1t_{2u}\downarrow$ will sometimes be of predominantly $4f$, and sometimes of predominantly $2p$ character. To deal with this difficulty, the occupation numbers were adjusted from iteration to iteration so as to ensure that the $4f\downarrow$-like orbital was always unoccupied. This procedure does not guarantee a good solution: if $4f$ and $2p$ eigenvalues lie too close together, there will inevitably be mixing in any numerical calculation, leading to charge transfer away from the Eu^{2+}, O^{2-} configuration, whatever occupation numbers are chosen. However, it does allow the solution to stabilize with $4f\downarrow$ either above or below $2p\downarrow$. When such stabilization was achieved, the $4f$ levels still continued to oscillate from iteration to iteration, over a range of ~0.1 a.u.; the calculation was terminated at a point close to the mean of the oscillation. The other valence levels were converged to within ±0.02 a.u.

The spin density from the SCF results is shown in Fig. 6. There is little change near the Eu site, as compared to the results from the "ionic" model potential (Fig. 4), but the s-p mixing and the associated complex density variations at the O site are much reduced. Since the SCF solution is not completely converged, the spin density at the O nucleus varies with the steady oscillation of eigenvalues over the iterations, on a range $(-0.016 \pm 0.004)a_0^{-3}$, and leads to a predicted hyperfine field of -8 ± 2 kG. It is interesting to note that one can find a roughly linear correlation between chalcogen hyperfine fields and empirical (Pauling) ionicity for those EuX compounds which have been measured.[12] This scheme predicts an EuO transferred hyperfine field of −10 kG, in reasonable agreement with our SCF results.

An altered spin density for the cluster with respect to the free ion will appear as an alteration

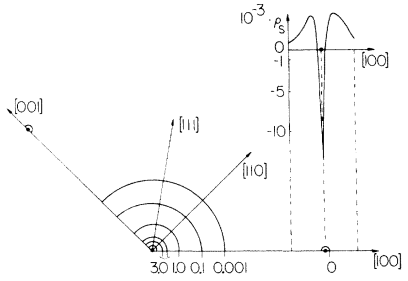

FIG. 6. Self-consistent spin-density contours for the $(EuO_6)^{10-}$ cluster in a fixed external potential, with $\alpha = 0.7$ (cf. caption of Fig. 3).

of the neutron magnetic form factor $f(k)$. The form factor has been measured for[13] EuO and found to differ from the free-ion HF value,[14] implying a more expanded spin density. This is attributed to relativistic effects, in analogy with similar results for Gd metal.[15] Form factors calculated by HFS-DVM for the Eu^{2+} free ion and for $(EuO_6)^{10-}$, in the isolated cluster model potential with $\alpha = 1.0$, were compared and found not to differ within the 1% accuracy of the calculated form factor values. However, when the SCF eigenfunctions were used to calculate a spherically averaged form factor, and compared to the results of a DVM free ion, $\alpha = 0.7$, treatment, a contraction in f was found, as shown in Fig. 7. The maximum difference between the two form factors is 2% of the maximum value of f, or about 4% of the magnitude of f for $(\sin\theta)/\lambda \approx 0.4$ Å^{-1}. In neither case is the HF-like experimental form factor reproduced, since the HFS approximation itself expands the spin density; but the prediction of a small

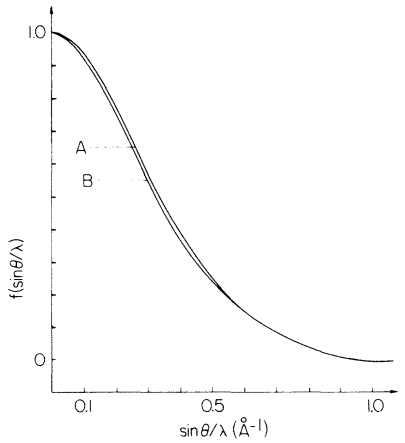

FIG. 7. Neutron magnetic form factors, calculated from HFS-DVM wave functions. Comparison between (A) the Eu^{2+} free ion, $\alpha = 0.7$ and (B) the $(EuO_6)^{10-}$ cluster, $\alpha = 0.7$, SCF results show that small solid-state bonding effects may be expected in EuO.

chemical effect suggests that the experimental deviation from the HF free-ion result, while surely including a relativistic contribution, may also reflect in part the solid-state environment of the ion.

V. PRESSURE DEPENDENCE OF THE ISOMER SHIFT IN EuS

The charge density at the Eu nucleus is accessible experimentally in the isomer shift between the Mössbauer spectra of Eu nuclei in different solid-state environments. Consider the emission of a photon of energy E_γ, for which the absorption by Eu nuclei in environment a is a maximum when the relative velocity of emitter and absorber is v_a, and in environment b when the velocity is v_b. Then the difference $\delta v = v_a - v_b$ may be written

$$\delta v = S'(Z)\frac{4\pi c Z e^2 R^2}{5E_\gamma}[\rho_a(0) - \rho_b(0)]\frac{\delta R}{R}$$
$$= \alpha \delta\rho(0) S'(Z), \tag{8}$$

where $e^2\rho_a(0)$ is the charge density at the Eu nucleus in environment a, R is the radius of the nucleus, δR is the change in that radius in the γ-ray transition, $S'(Z)$ is a relativistic correction factor, and α is the isomer-shift calibration constant. The S' factor was originally based[16] on an approximate proportionality between the relativistic and nonrelativistic *hydrogenic* charge densities. In this work it is replaced by the value (2.9) for Eu derived from a direct comparison of Dirac-Fock and HF free-atom calculations.[17,18]

The measured effect is of course a product of nuclear and solid-state factors, both unknown. If, however, $\delta\rho(0)$ can be ascertained by calculation, $\delta R/R$ can be obtained by comparison with experiment. The molecular-cluster model is well adapted to the treatment of the covalent effects of the environment on $\rho(0)$.[18] Many-electron effects may be important for $\rho(0)$, so that comparisons between different ions (e.g., Eu^{2+} and Eu^{3+}) should not be made in a one-electron approximation. However, where no major rearrangement of the charge density occurs, many-electron terms will change little, and $\delta\rho(0)$ will be dominated by covalent effects (small charge transfers into and out of valence s orbitals, and changes in their shapes). These effects are described by one-electron theories, such as HFS. One such situation where the density is not drastically altered is found in the pressure dependence of the isomer shift in a given compound.

The pressure dependence of both isomer shift and hyperfine splitting in the Mössbauer spectra has been measured for EuS.[2] As the pressure is increased from 9 to 87 kbar, the Eu–S bond length decreases from 5.64 to 5.35a_0,[8] and the isomer shift changes by 1.1 mm/sec, in a sense indicating increased charge density at the Eu nucleus. The magnitude of the (negative) hyperfine field also increases with increasing pressure.

Calculations were performed on the $(EuS_6)^{10-}$ cluster, in the isolated cluster model potential, with $\alpha = 1$, for several bond lengths. In order to provide maximum variational freedom, the Eu s-basis set was expanded as indicated in Table I. The number of integration points was increased to 6400 (half of which were within $r < 0.03$) to treat the core region more accurately. Unfortunately, core molecular-orbital contributions to $\rho(0)$ were unstable against integration grid and basis set changes in the fifth or sixth decimal figure due to a combination of residual integration error and propagation of noise in solving the matrix secular equation. Therefore, core molecular-orbital contributions were omitted, and the systematic trend of the valence density is displayed in Fig. 8.

The total change $\delta\rho(0)$ is $0.79a_0^{-3}$. Multiplying by $S'(Z) = 2.9$ and comparing this relativistically corrected value with the measured isomer shift of 1.1 mm/sec, gives a calibration factor α of $-0.48a_0^3$ mm/sec. A value for α of $-0.35a_0^3$ mm/sec has previously been obtained,[19] by comparing the relativistic charge densities calculated for free Eu^{2+} and Eu^{3+} ions, with the isomer shift between typical divalent and trivalent Eu compounds. The inclusion of an Eu core contribution to $\delta\rho(0)$ will probably reduce our value of α. Further desirable corrections include a self-consistent treatment, to discover the effects of altered shielding of the core by hybridized valence functions. Also, the existence of relativistic free-ion calculations makes it possible to apply relativistic corrections orbital by orbital, since the or-

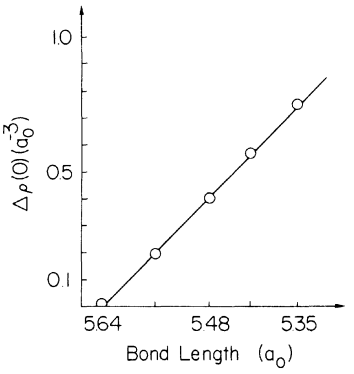

FIG. 8. Variation of the charge density at the Eu nucleus in the $(EuS_6)^{10-}$ cluster as a function of the Eu–S bond length. Solid line is the best fit to the calculated points (circles).

bitals contribute in different proportions to $\rho(0)$. This technique has been applied to Fe.[20] A fully relativistic (Dirac-Slater) cluster calculation would be better yet.

VI. EIGENVALUES AND EXCITED STATES

Empirical energy-level schemes have been constructed for EuO and EuS which are consistent with a number of experiments.[1] The separation of the filled $4f\uparrow$ levels from the conduction band was taken from the optical absorption edge,[21] and the relative positions of the $4f\uparrow$ and ligand p levels were taken from the ultraviolet photoemission spectrum.[22] In the resulting *one-electron* scheme the $4f\uparrow$ levels lie in the gap between the valence (ligand p) and conduction (Eu $5d$, $6s$) bands. Soft-x-ray emission and absorption spectra have been interpreted as confirmation of this arrangement.[23]

Three theoretical determinations of one-electron energy levels in europium chalcogenides have previously been made: an estimate of the effects of the Madelung potential, polarization, and overlap effects on Eu and ligand free-atom levels,[24] an augmented-plane-wave (APW) band calculation,[3] and an orthogonalized-plane-wave (OPW) treatment.[4] All of these calculations are in qualitative agreement with the empirical levels scheme: none was carried to self-consistency.

Despite the apparent success of these models, caution must be exercised in comparing one-electron eigenvalues of any model Hamiltonian with experimental spectra, which measure total energy differences. Intra-atomic correlation effects give rise to splittings observable in free ions and in ionic crystals like EuO.[25] Further correlation effects can be crudely represented as state-dependent Coulomb energy shifts. The importance of these effects for such highly localized states as $4f$ levels is very well known[1,26]; producing relative shifts between $4f$ and valence levels of the order of 10 eV: it is even evident among $3d$ electrons in such systems as VO.[27]

There appears to be no satisfactory one-electron approach which will yield a *single* set of self-consistent wave functions for describing both the optical and the ionizing transitions. The ionization energies of the electrons differ from the one-electron eigenvalues ϵ_i, and the transition energies from the $\epsilon_i - \epsilon_j$ because of the relaxation of final-state wave functions, as well as Coulomb correlation effects. Relaxation effects in the Eu chalcogenides should be important for the localized $4f$ orbitals, and small for the more extended ligand p states. Further, while the HF eigenvalues are equal, by Koopman's theorem, to the unrelaxed ionization energies, this is not true of the HFS eigenvalues; a so-called "Koopmans correction" must also be included. If the difference in total energies of initial (N electron) and final ($N-1$ electron) states are expanded in a Taylor series in the occupation numbers q_i, it may be shown that relaxation and Koopmans corrections are included to second order in q_i, if the HFS equations are solved for a transition state, which the ionized level has $q_N = 0.5$. This or more thorough procedures may give ionization energies whose ordering in energy is different from that of the eigenvalues.[5,31] And of course a new calculation is necessary for each transition.

It has been shown by Cho[3] that the Eu $4f$ level in particular is extremely sensitive to the choice of α in the HFS approximation, varying by ~0.7 Hartree atomic units (a.u.) for $\frac{2}{3} \leq \alpha \leq 1$. For some values of α, the $4f\uparrow$ level lies above the ligand p band; for others, below it. Cho was able to obtain reasonable agreement between APW band structure and the empirical level scheme, by a suitable choice of α. In fact, different α values were selected for different regions of the crystalline unit cell. In view of the corrections noted above, this procedure must be considered to be semiempirical.

A. Core eigenvalues and spin splittings

The eigenvalues and spin splittings for the Eu core levels are given in Table II for both the ionic crystal potential and the self-consistent field. The splittings, which differ little in the cluster from the free ion, may be compared to structure found in experimental binding energies, if final-state effects are neglected. From soft-x-ray spectra[23] the $3d$ level is found to have a spin-splitting of ~0.16 a.u., compared to calculated values of 0.12 ($\alpha = 1.0$) and 0.08 a.u. ($\alpha = 0.7$). This level, or rather a suitable average of its spin-orbit-split components, lies 41.75 a.u. below the $4f\uparrow$ level, compared to calculated values of 42.90 a.u. ($\alpha = 1$) and 41.28 a.u. ($\alpha = 0.7$) in the model potentials, and 41.42 a.u. ($\alpha = 0.7$) in SCF. There are no other experimental measurements of core splittings in EuO, but in trivalent Eu compounds, a splitting of 7 eV has been found for the $4s$ level by ultraviolet photoemission spectroscopy,[28] in agreement with the value calculated for $\alpha = 0.7$. A complex structure is found for the $4d$ level.[29] The experimental data reflect many-electron and relaxation effects in the spin splittings of actual transitions, which can give results different from spin-unrestricted HFS or HF predictions, even in atomic models.[30]

B. Valence levels from free-atom/ion potentials

Among the valence levels also, the spin-splittings are expected to resemble the free-ion $Eu^{2+}(4f\uparrow)^7$ results, with rather small changes due to charge transfer and hybridization effects. In the model-potential results, the effects of ligand polarization have not yet entered the potential. For $(EuS_6)^{10-}$ the eigenvectors composed of predominantly Eu basis functions have the appropriate free-ion splittings, and the sulfur states are not split by more than 0.001 a.u. The $(EuO_6)^{10-}$ results for several model potentials are shown in Figs. 9 and 10. The labels in these figures refer to atomic states, and the levels actually shown are chosen so far as possible from eigenvectors of pure atomic character (e.g., for the $4f$ levels, the a_{2u} eigenvalue is used). The Eu $5p$ level shows anomalous spin splittings, symptomatic of strong mixing with the O $2s$ basis functions. In the "neutral" crystal potential the $4f$ splitting is similarly affected by mixing with the O $2p$ functions, in the t_{1u} and t_{2u} representations, as discussed in Sec. IV. The crystal-field splittings of the valence levels are suppressed. They are not given very consistently by the results for the various model potentials, partly because they occur at the limits of accuracy of the calculation, and partly because of the effects of hybridization. In several of the calculations for EuO, two $5d$ functions were added to the Eu basis set (see Table I), so that cluster "$5d$" levels were also obtained. Thus, a crude estimate of the crystal-field splitting may be made, i.e., $\Delta_{5d} = \epsilon\uparrow(e_g) - \epsilon\uparrow(t_{2g}) = 0.03$ a.u. (in an isolated cluster, for $\alpha = 1.0$) and 0.06 a.u. (in the neutral crystal potential for $\alpha = 0.75$), compared to a measured value of 0.12 a.u.[25]

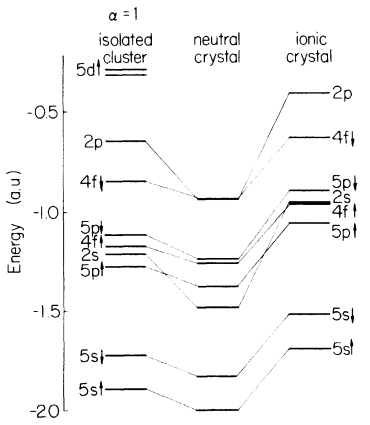

FIG. 9. Valence eigenvalues of the $(EuO_6)^{10-}$ cluster in various model potentials with $\alpha = 1$. Levels are labeled by atomic type (Eu $5s$, $5p$, $5d$, and $4f$, and O $2s$ and $2p$). Hybridization and crystal-field effects generate splittings of the $2s$, $2p$, and $4f$ levels, which are not shown.

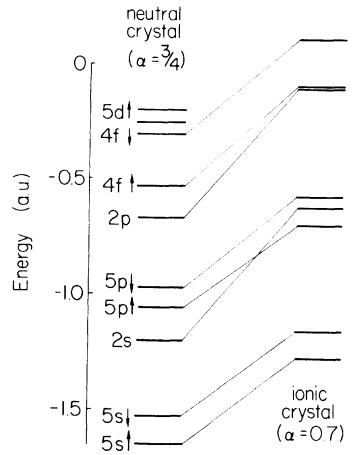

FIG. 10. Valence eigenvalues of the $(EuO_6)^{10-}$ cluster (cf. Fig. 9) for reduced values of α. Note the reordering of the levels compared with Fig. 9.

C. Comparison to band-theory results

Since the eigenvalues are so dependent on the model potential, a comparison to previous work must use a closely similar potential. In the OPW case, pseudopotential terms would have to be included: this has not been done. For the APW results, a suitable potential has already been described. While Cho[3] used an "ionic" crystal potential with exchange parameters $\alpha(\text{Eu}) = 0.75$ and $\alpha(\text{O}) = 1.0$, his muffin-tin approach removes the asphericity, especially that due to the Madelung potential, so that "neutral" and "ionic" APW results differ by little more than an overall shift. The comparison is thus made to the results for $(EuO_6)^{10-}$ in the "neutral" crystal potential, with $\alpha = \frac{3}{4}$. The separations of the $2p$, $4f\uparrow$, and $2p$ states in the cluster case (including hybridization effects) are about $\frac{1}{2}$ of the APW widths. This is to be expected, since the smaller manifold of states in the cluster allows less mixing and consequently less broadening than in the band calculation. The variation of the position of the $4f\uparrow$ level with α also agrees with the APW results. The $5d$ orbital is not well treated by the cluster approach, since it forms a broad band due to overlap with the $4f$ orbitals on other Eu ions. (Part of the band width could be obtained by adding nearest-neighbor Eu sites to the cluster.) The cluster $5d$ level is too high, giving a $4f\uparrow$ to $5d\uparrow$ gap of 0.28 a.u. compared to the APW (and experimental) value of 0.04 a.u. However, it may be noted that the APW d bands are quite wide (~0.2 a.u.), and the molecular or-

TABLE IV. SCF valence eigenvalues and spin splittings (in a.u.) for the $\alpha=0.7$ $(EuO_6)^{10-}$ cluster in external ionic crystal potential. Values of ϵ given as +0.017, etc., indicate levels unbound with respect to the zero of the potential used.

Molecular orbital	$\epsilon\uparrow$	$\epsilon\downarrow$	$\Delta\epsilon$	Atomic orbital
$6a_{1g}$	1.162	1.051	0.111	5s
$5t_{1u}$	0.585	0.504	0.081	5p
$7a_{1g}$	0.408	0.405	0.002	2s
$4e_g$	0.400	0.398	0.001	2s
$6t_{1u}$	0.394	0.385	0.009	2s
$7t_{1u}$	+0.017	+0.230	0.213	4f
$1a_{2u}$	+0.018	+0.222	0.203	4f
$1t_{2u}$	+0.019	+0.226	0.207	4f
$8a_{1g}$	+0.087	+0.095	0.008	2p
$8t_{1u}$	+0.096	+0.100	0.004	2p
$3t_{2g}$	+0.096	+0.098	0.002	2p
$2t_{2u}$	+0.110	+0.109	−0.001	2p
$1t_{1g}$	+0.118	+0.120	0.002	2p
$5e_g$	+0.126	+0.128	0.002	2p
$9t_{1u}$	+0.131	+0.128	0.003	2p

bital $4t_{2g}$ may be supposed to lie at the center of such a band. In the results of Cho, the center of the Γ'_{25} band (corresponding to the $4t_{2g}$ molecular orbital) lies about 0.3 a.u. above the $4f\uparrow$ band, in reasonable agreement with the molecular-orbital result. Thus, there is a rather good agreement between the cluster and APW results calculated in similar potentials. However, where the "ionic" crystal potential is used, the Eu core levels are shifted by 0.31 a.u. and the O core level (1s) by 0.54 a.u. This relative shift is apparent in the valence levels as shown in Fig. 9 for $\alpha=1$ and in Fig. 10 for smaller values of α.

D. Self-consistent cluster eigenvalues

The valence eigenvalues obtained in the self-consistent treatment of the $(EuO_6)^{10-}$ cluster are given in Table IV. The spin splittings of the Eu levels are reduced below free-ion and model-potential cluster results, and splittings of the order of 0.001 a.u. are induced in the O ligand levels. The most important feature of the results, however, is that the SCF $4f\uparrow$ level lies below the ligand $2p$, in contradiction of the empirical and APW and OPW energy-level schemes. This result conflicts with the observed photoemission spectrum, to the extent that *ground-state* HFS levels may be said to predict ionization energies. It has already been noted, however, that various corrections to the HFS levels may be necessary. Although it is expected that the ionization energy of the $4f\uparrow$ level will be decreased by relaxation, compared to the $2p$, it is not clear that the required reversal of levels will be achieved by cluster transition-state calculations. A crude estimate based on the comparison of $4f$ eigenvalues in $4f^6$ and $4f^7$ configurations of Eu^{2+} and of $2p$ eigenvalues in the O atom and O^{2-} ions indicates that it will not. Many-electron effects in the $4f$ levels will be important. It is clear that corrections to the SCF-HFS levels are significant in the Eu chalcogenides, and cannot be avoided by varying α in a model-potential calculation to reproduce the empirical energy-level scheme.

VII. CONCLUSION

The local properties of EuO and EuS have been examined in a molecular-cluster model. The HFS approximation has been applied to calculate the ground-state properties of the clusters, for which it is appropriate. Comparisons have been made to experiment and to other theoretical approaches.

With respect to excited states, it has been shown that model-potential cluster calculations yield eigenvalues in agreement with model-potential APW theory. These eigenvalues are consistent with a one-electron interpretation of EuO spectra. But ground-state HFS eigenvalues do not, in principle, give the one-electron excitation spectrum, nor may many-electron effects be ignored in transitions involving the $4f$ shell. Extension of the HFS calculation to self-consistency shows that it does not in fact predict the excitations; both relaxation and correlation must be included in the theory of the spectra.

*Research supported by NSF (through the Northwestern University Materials Research Center) and the AFOSR Grant No. AFOSR 71-2012G. Part of this work represents a thesis submitted by E. Byrom to the Physics Dept., Northwestern University, in partial fulfillment of the requirements for the Ph.D. degree.

[1]S. Methfessel and D. C. Mattis, in *Handbuch der Physik* (Springer-Verlag, Berlin, 1968), Vol. 18/1.

[2]U. F. Klein, G. Wortmann, and G. M. Kalvius, Proc. ICM-73 (Moscow) IV, 149 (1974); C. Sauer, U. Kobler, W. Zinn, and G. M. Kalvius (unpublished); G. M. Kalvius, U. F. Klein, and G. Wortmann, J. Phys. (Paris) 35, C6-139 (1975).

[3]S. J. Cho, Phys. Rev. 157, 632 (1967); *ibid.* B 1, 4589 (1970).

[4]K. Lendi, Phys. Kondens. Mater. 17, 189 and 215 (1974).

[5]For an extended discussion of the local exchange ap-

proximation, see J. C. Slater, *Quantum Theory of Molecules and Solids* (McGraw-Hill, New York, 1974), Vol. IV, Chaps. 1–3.

[6]D. E. Ellis, Int. J. Quantum Chem. Symp. 2, 35 (1968); D. E. Ellis and G. S. Painter, Phys. Rev. B 2, 2887 (1970); T. Parameswaran and D. E. Ellis, J. Chem. Phys. 58, 2088 (1973).

[7]R. W. G. Wyckoff, *Crystal Structures* (Wiley, New York, 1963), Vol. 1, 2nd ed., p. 87.

[8]F. Levy and P. Wachter, Solid State Commun. 8, 183 (1970).

[9]E. Byrom and D. E. Ellis (unpublished results).

[10]P. S. Bagus and A. J. Freeman (unpublished results).

[11]J. M. Baker and J. P. Hurrell, Proc. Phys. Soc. (London) 82, 742 (1963).

[12]K. Raj, J. I. Budnick, and T. J. Burch, Bull. Am. Phys. Soc. 20, 291 (1975); J. I. Budnick (private communication).

[13]W. C. Koehler and J. W. Cable (unpublished).

[14]M. Blume, A. J. Freeman, and R. E. Watson, J. Chem. Phys. 37, 1245 (1962); *ibid.* 41, 1878 (1964).

[15]A. J. Freeman and J. P. Desclaux, Int. J. Magn. 3, 311 (1972).

[16]D. A. Shirley, Rev. Mod. Phys. 36, 339 (1964).

[17]J. P. Desclaux and A. J. Freeman (unpublished).

[18]The various approaches which have been made are the subject of a recent review by A. J. Freeman and D. E. Ellis [J. Phys. (Paris) 35, C6-3 (1975)].

[19]R. Bauminger, G. M. Kalvius, and I. Nowik, in *Mössbauer Isomer Shifts*, edited by G. K. Shenoy and F. E. Wagner (North-Holland, Amsterdam, 1975), Chap. 10.

[20]A. Trautwein, F. E. Harris, A. J. Freeman, and J. P. Desclaux, Phys. Rev. B 11, 4101 (1975).

[21]J. O. Dimmock, IBM J. Res. Dev. 14, 301 (1970).

[22]D. E. Eastman, F. Holtzberg, and S. Methfessel, Phys. Rev. Lett. 23, 226 (1969); G. Busch, P. Cotti, and P. Munz, Solid State Commun. 7, 795 (1969); P. Cotti and P. Munz, Phys. Kondens. Mater. 17, 307 (1974).

[23]J.-M. Mariot and R. C. Karnatak, Solid State Commun. 16, 611 (1975).

[24]T. Kasuya, J. Appl. Phys. 41, 1090 (1970).

[25]J. Feinleib, W. J. Scouler, J. O. Dimmock, J. Hanus, T. B. Reed, and C. R. Pidgeon, Phys. Rev. Lett. 22, 1385 (1969); M. J. Freiser, S. Methfessel, and F. Holtzberg, J. Appl. Phys. 39, 900 (1968).

[26]A. J. Freeman, in *Magnetic Properties of Rare Earth Metals*, edited by R. J. Elliott (Plenum, New York, 1972), Chap. 6 and references therein; J. F. Herbst, D. N. Lowy, and R. E. Watson, Phys. Rev. B 6, 1913 (1972).

[27]J. B. Goodenough, in *Annual Reviews of Materials Science*, edited by R. A. Huggins, R. H. Bube, and P. W. Roberts (Annual Reviews, Palo Alto, 1971), Vol. 1, p. 101; and in *Progress in Solid State Chemistry*, edited by H. Reiss (Pergamon, Oxford, 1971), Vol. 5, p. 145.

[28]R. L. Cohen, G. K. Wertheim, A. Rosencwaig, and J. J. Guggenheim (unpublished results cited by Herbst *et al.*, Ref. 26).

[29]C. Bonnelle, R. C. Karnatak, and C. K. Jorgensen, Chem. Phys. Lett. 14, 145 (1972).

[30]A. J. Freeman, P. S. Bagus, and J. V. Mallow, Int. J. Magn. 4, 35 (1973); P. S. Bagus, A. J. Freeman, and F. Sasaki, Int. J. Quantum Chem. Symp. 7, 83 (1973); and Phys. Rev. Lett. 30, 850 (1973).

[31]A. Rosén and D. E. Ellis, J. Chem. Phys. 62, 3039 (1975).

[32]E. Clementi, IBM J. Res. Dev. 9, 2 (1965); see especially *Tables of Atomic Functions*.